

1 For submission to *Molecular Therapy – Oncolytics*

2

3 **Oncolytic effect of Newcastle Disease Virus is associated with interferon pathway  
4 expression in canine mammary cancer cell lines.**

5

6 Mariana R. Santos<sup>1</sup>, Pedro L.P. Xavier<sup>1</sup>, Pedro R.L. Pires<sup>1</sup>, Arina L. Rochetti<sup>1</sup>, Daniele  
7 Rosim<sup>1</sup>, Muhammad Munir<sup>2</sup>, Helena L. Ferreira<sup>3</sup>, Heidge Fukumasu<sup>1\*</sup>.

8

9 <sup>1</sup> Laboratory of Comparative and Translational Oncology, Department of Veterinary  
10 Medicine, School of Animal Science and Food Engineering, University of Sao Paulo, Av.  
11 Duque de Caxias Norte n°225, Pirassununga 13635-900, Sao Paulo, Brazil.

12 <sup>2</sup> Division of Biomedical and Life Sciences, Lancaster University, Lancaster, LA1 4YG,  
13 United Kingdom.

14 <sup>3</sup> Department of Veterinary Medicine, School of Animal Science and Food Engineering,  
15 University of Sao Paulo, Av. Duque de Caxias Norte n°225, Pirassununga 13635-900,  
16 Sao Paulo, Brazil.

17

18 \*Correspondence to: Heidge Fukumasu, email: [fukumasu@usp.br](mailto:fukumasu@usp.br)

19

20

21

22   **Abstract**

23   Canine Mammary Carcinomas (CMC) are one of the major health threats in dogs,  
24   globally accounting for about 40% of all tumors in intact females and being malignant in  
25   half of the cases. The oncolytic virotherapy is a promising strategy to treat canine as well  
26   as human cancer patients with non-pathogenic replicating viruses. Here we evaluated the  
27   antitumor activity of one lentogenic, non-lytic NDV LaSota strain expressing GFP  
28   (NDV-GFP) on 5 different CMC (2 epithelial-like and 3 mesenchymal-like) and one non-  
29   tumorigenic cell line, regarding cell viability, cell death, selectivity index, morphology  
30   and transcriptome analysis. As evidenced by the selectivity index, all CMC cell lines were  
31   more susceptible to NDV-GFP than the normal cells ranging from ~3.1x to ~78.7x. The  
32   oncolytic effect of NDV-GFP was more evident in cell lines with mesenchymal-like  
33   instead of epithelial-like phenotype. Also, there was an inverse association of IFN  
34   pathway expression and selective oncolysis of NDV, demonstrating this mechanism as  
35   the most prominent for oncolysis by NDV. To our knowledge, this is the first description  
36   of oncolysis by an NDV strain in canine mammary cancer cells. We also demonstrated  
37   specific molecular pathways related to NDV susceptibility in these cancer cells, opening  
38   the possibility of using NDV as therapeutic-targeted option for more malignant CMCS.  
39   Therefore, these results greatly urge for more studies using oncolytic NDVs, especially  
40   considering genetic editing to improve efficacy in dogs.

41

42

43   **Keywords:** epithelial-mesenchymal transition; comparative oncology; selectivity index;  
44   RNA-seq; Paramyxovirus

45     **Introduction**

46

47         Canine Mammary Carcinomas (CMC) are one of the major health threat in dogs,  
48     globally accounting for about 40% of all tumors in intact females, and being malignant  
49     in half of the cases (SLEECKX et al., 2011). The standard treatment for small animals  
50     with CMTs is surgery and adjuvant therapies (e.g. post-operative chemotherapy) can be  
51     advocated for dogs with advanced disease. But adjuvant therapies have demonstrated  
52     limited effects on prognosis and a surplus at treatment-related side effects in patients with  
53     CMTs (SLEECKX et al., 2011). Since current adjuvant therapies in veterinary medicine  
54     are insufficient to treat advanced stages of CMC, the development of new and improved  
55     therapeutic options is in a high demand to reduce cancer patient's mortality.

56

57         The Oncolytic Virotherapy is a promising strategy to treat canine as well as human  
58     cancer patients with non-pathogenic replicating viruses (SÁNCHEZ et al., 2018).  
59     Oncolytic Viruses (OVs) are natural or engineered infectious agents that show three  
60     fundamental mechanisms of action: (i) tumor selective infection, replication and spread  
61     after direct oncolysis; (ii) tumor microenvironment reshape, and (iii) tumor-associated  
62     antigens release and trigger of adaptive anti-tumor immune responses (ENGELAND;  
63     BELL, 2020). These principles end up in tumor vaccination effects, prompting  
64     therapeutic and protective antitumor immunity with minimal toxicity to normal cells,  
65     hence fewer side effects than conventional cancer treatments (RUSSELL; BARBER,  
66     2018; ENGELAND; BELL, 2020).

67

68         A recent review on OVs considered the Newcastle Disease Virus (NDV) as a  
69     breakthrough for improvements in cancer therapy (SCHIRRMACHER; VAN GOOL;  
70     STUECKER, 2019). This virus features a natural preference for replication in many  
71     tumor cells comparing to normal cells and the observed antitumor effect of NDV appears  
72     to be a result of both selective killing of tumor cells and induction of immune responses  
73     (ZAKAY-RONES; TAYEB; PANET, 2015). Although cells of various human tumors  
74     were sensitive for NDV, only one study demonstrate the potential of NDV as oncolytic  
75     for canine lymphoma cells (SÁNCHEZ et al., 2015). Therefore, here we evaluated the  
76     antitumor activity of one lentogenic recombinant NDV LaSota strain expressing the GFP  
77     protein (NDV-GFP) on 5 different canine mammary cancer cell lines and one non-

78 tumorigenic cell line and demonstrated that the loss of Interferon pathway response was  
79 the main pathway associated with the oncolytic effects of NDV.

80

81 **Material and Methods**

82

83 **Cell lines**

84 Five canine mammary cancer cell lines (CMC) were used in this experiment: E20, E37,  
85 M5 and M25 cell lines were isolated and established in our laboratory as previously  
86 described (CORDEIRO et al., 2018; XAVIER et al., 2018). The CF41.Mg cell line was  
87 kindly provided by Dr. Debora A. P. C. Zuccari (Faculdade de Medicina de São José do  
88 Rio Preto, São José do Rio Preto, São Paulo, Brazil). The E20 and E37 cell lines presented  
89 an epithelial-like morphology whereas the M5, M25 and CF41.Mg presented a  
90 mesenchymal-like morphology (XAVIER et al., 2018). The canine embryonic fibroblasts  
91 were kindly provided by Dr. Carlos Eduardo Ambrósio (Laboratório de Cultivo de  
92 Células Tronco e Terapia Gênica, Faculdade de Zootecnia e Engenharia de Alimentos,  
93 Pirassununga, São Paulo) (GONÇALVES et al., 2017). All CMC cells were maintained  
94 in 75 cm<sup>2</sup> flasks at 37°C and 5% CO<sub>2</sub> with Dulbecco's Modified Eagle Medium: Nutrient  
95 Mixture F-12 (DMEM-F12) supplemented with 10% fetal bovine serum and 1%  
96 antibiotic/antimycotic. The canine embryonic fibroblasts were cultured with Dulbecco's  
97 Modified Eagle Medium: Nutrient Mixture F-12 (DMEM-F12) supplemented with 15%  
98 fetal bovine serum, 1% of glutamine and 1% antibiotic/antimycotic. Passaging was  
99 performed when cells were 70-80% confluent. Culture evolution was evaluated daily by  
100 optical microscopy (Axio Vert A1, Zeiss, Germany). All reagents used for cell culture  
101 were purchased from Thermo Fisher Scientific, USA.

102

103 **Virus titration and morphological analysis**

104 A genetically modified NDV La Sota strain, a genotype II class II NDV, expressing GFP  
105 (AL-GARIB et al., 2003), was kindly provided by Dr. Muhammad Munir (Lancaster  
106 University, England). Virus titers were obtained by calculating the median tissue culture  
107 infectious dose per ml (TCID<sub>50</sub>/ml) using Reed and Muench method (REED; MUENCH,  
108 1938). Briefly, M25 cells were seeded at 3,000/well in 96 well plates containing 100 µl  
109 of supplemented media as described. After 24h, media was removed and each well was  
110 washed with PBS. The cells were exposed to different concentrations of the virus (10<sup>-11</sup>  
111 a 10<sup>-1</sup>). After 90 minutes, 100 µl of medium supplemented with 2% of FBS and 1%

112 antibiotic/antimycotic were added in each well. The cytopathic and morphologic effects  
113 were evaluated daily for 5 days. Pictures were taken with optical and fluorescence  
114 microscopy using ZEISS—Axio Vert A1 with a camera Axio Can 503 attached using a  
115 520 nm wavelength filter for green color (ZEISS, GER).

116

117 **DNA sequencing of the NDV fusion gene**

118 DNA sequencing was done to confirm the cleavage site sequence. Viral RNA  
119 purifications were performed with QIAamp Viral RNA Mini Kit (Qiagen, Hilden,  
120 Germany), according to manufacturer's instructions, followed by RT-PCR using  
121 SuperScript1 III One- Step RT-PCR System with Platinum1 Taq DNA Polymerase (Life  
122 Technologies, Carlsbad, CA, USA) and previously described 4331F/5090R primers  
123 (MILLER et al., 2015). Amplicons were visualized in 2% of SYBR Safe (Life  
124 Technologies, Carlsbad, CA, USA) low Melting Point Agarose (Life Technologies,  
125 Carlsbad, CA, USA). Products were purified using Illustra GFX PCR DNA and Gel Band  
126 Purification Kits (GE Health Care and Life Sciences, Buckinghamshire, England). DNA  
127 sequencing was performed with BigDye Terminator v3.1 Cycle Sequencing Kit (Life  
128 Technologies, Carlsbad, CA, USA) in ABI 3730XL DNA Analyzer (Applied Biosystems,  
129 Foster City, CA USA) at CEGH-CEL facility (IB-USP). The obtained sequences were  
130 evaluated for quality using the Sequence Scanner™ Software 2 (Applied Biosystems,  
131 Foster City) and edited by MEGA7 (KUMAR; STECHER; TAMURA, 2016).  
132 Afterwards, the obtained sequences and sequences available in GenBank were aligned  
133 using Clustal W (THOMPSON; HIGGINS; GIBSON, 1994) and Bioedit Sequence  
134 Alignment software version 7.2.5. (HALL, 1999). The cleavage site was deduced based  
135 on criteria utilized by OIE to assess virulence of NDV isolates (OIE, 2012).

136

137 **Virus infection and replication in cell lines**

138 The CMC cells and canine embryonic fibroblasts were seeded at 5,000 cells per well in  
139 96 well plates containing 100 µl of supplemented media as described. After 24h, media  
140 was removed, each well was washed with PBS and new culture media containing  $10^2$  to  
141  $10^{-5}$  MOI of NDV-GFP was added. After 90 minutes, 100 µl of media supplemented with  
142 2% of FBS and 1% antibiotic/antimycotic was added in each well. Then, cell lines were  
143 evaluated up to 72 hours for the detection of GFP expression due to virus replication and  
144 gene expression.

145

146 **NDV cytotoxic assay**

147 The CMC cells and canine embryonic fibroblasts were seeded at 5,000 cells per well in  
148 96 well plates containing 100 µl of supplemented media as described. After 24h, media  
149 was removed, each well was washed with PBS and new culture media containing different  
150 concentrations of MOI ( $10^2$  to  $10^{-5}$ ) was added using the NDV-GFP. After 90 minutes,  
151 100 µl of media supplemented with 2% of FBS and 1% antibiotic/antimycotic was added  
152 in each well. After 72h, cells were fixed using 4% paraformaldehyde for 10 minutes and  
153 stained with 2% crystal violet for 20 minutes. Acetic acid (10%) was added to dissolve  
154 the crystals. Optical density at 540 nm was measured in a Fluorstar Optima (BMG  
155 Labtech, Germany). The selectivity index (SI) was calculated using the half maximal  
156 inhibitory concentration (IC<sub>50</sub>) of each cancer cell line in comparison to the non-  
157 tumorigenic cell line.

158

159 **Cell death assay**

160 The CMC cells and canine embryonic fibroblasts were seeded at 5,000 cells per well in  
161 96 well plates. After 24h, cells were treated with the NDV-GFP IC<sub>50</sub> for 72h. A dye mix  
162 containing 100 µg/ml of acridine orange and 100 µg/ml of ethidium bromide was added  
163 to cells and observed for fluorescence emission using ZEISS—Axio Vert A1 with a  
164 camera Axio Can 503 attached using a 520 nm and 620 nm wavelength filter for green  
165 and red colors, respectively. Analysis were performed in triplicate, counting at least 100  
166 cells each. The results were analyzed based on the arrangement of chromatin to  
167 differentiate apoptotic, oncotic and live cells (RIBBLE et al., 2005). Live cells have  
168 normal nuclei staining which presents green chromatin with organized structures.  
169 Apoptotic cells contain condensed or fragmented chromatin (green or orange) and oncotic  
170 cells have similar normal nuclei staining as live cells except the chromatin is orange  
171 instead of green (RIBBLE et al., 2005).

172

173 **Total RNA extraction, RNA-sequencing and data analysis**

174 Four cell lines (E20, CF41.Mg, M25 and M5 but not E37 and control cells) were analyzed  
175 by RNA-seq before exposure to the virus to evaluate the possible biological processes  
176 associated with the oncolytic effects of the virus. The total RNA of triplicates of  $10^6$  cells  
177 of each of the four CMC cell lines was extracted using RNeasy Mini Kit (QIAGEN, UK).  
178 The RNA quality and quantity were assessed using automated capillary gel  
179 electrophoresis on a Bioanalyzer 2100 with RNA 6000 Nano Labchips according to the

180 manufacturer's instructions (Agilent Technologies, Ireland). Only samples that presented  
181 an RNA integrity number (RIN) higher than 8.0 were considered to the sequencing. RNA  
182 libraries were constructed using the TruSeq™ Stranded mRNA LT Sample Prep Protocol,  
183 then each library were analyzed by bioanalyzer for quality and sequenced on Illumina  
184 HiSeq 2500 equipment in a HiSeq Flow Cell v4 using HiSeq SBS Kit v4 (2x100pb).  
185 Sequencing quality was evaluated using the software FastQC  
186 (<https://www.bioinformatics.babraham.ac.uk/projects/fastqc/>) and no additional filter  
187 was performed. Sequence alignment against the canine reference genome (CanFam3.1)  
188 was performed using STAR (DOBIN et al., 2013), according to the standard parameters  
189 and including the annotation file (Ensembl release 89). Secondary alignments, duplicated  
190 reads and reads failing vendor quality checks were removed using Samtools (LI et al.,  
191 2009). Alignment quality was confirmed using Qualimap (GARCÍA-ALCALDE et al.,  
192 2012). Gene expression was estimated by read counts using HTseq (ANDERS; PYL;  
193 HUBER, 2015). Count were normalized by Variance-stabilizing Transformation (VST)  
194 and differential expression analysis (DE) was performed using DeSeq2 package (LOVE;  
195 HUBER; ANDERS, 2014) and the Benjamini-Hochberg procedure was used to calculate  
196 the false discovery rate (FDR) and transcripts presenting FDR  $\leq 0.01$  and log-fold change  
197 (LogFC)  $> 1$  were considered differential expressed.

198

## 199 Statistical Analysis

200

201 The IC50 was calculated by a nonlinear regression and the apoptotic index was analyzed  
202 using Two-way ANOVA. GraphPad Prism version 8.0.0 for Mac (GraphPad Software,  
203 USA) was used for statistical analysis and graph preparation.

204

205

## 206 Results

207

### 208 NDV-GFP titration and cleavage site sequencing

209 The obtained titer of NDV-GFP in M25 cells was  $10^{5.86}$  TCID<sub>50</sub>/ml after 5 days post-  
210 infection. The cleavage site sequence from the virus confirmed to be <sup>113</sup>RQGR\*L<sup>117</sup>,  
211 which is specific for lentogenic viruses based on criteria utilized by OIE to assess  
212 virulence of NDV isolates.

213

214

215 **Morphological effects of NDV-GFP in Canine Mammary Cancer cell lines**

216 The time that GFP was visualized varied between cell lines, being the M5 cell line  
217 the first where GFP (20h) was visualized and the E20 the last (48h, table 1). The other 3  
218 cell lines (M25, Cf41.Mg and E37) and normal cells (fibroblasts) have GFP detected at  
219 24h after the exposure to NDV-GFP. The viral infection didn't induce the formation of  
220 syncytia in the cell lines as expected since the virus is a lentogenic strain.

221

222 **Cytotoxicity of NDV-GFP in CMC cell lines**

223 The cytotoxic potential of NDV-GFP in all CMC cell lines and normal cells was  
224 evaluated by the comparison of IC<sub>50</sub> for each cell line (Table 1). As evidenced by the  
225 selectivity index, all CMC cell lines were more susceptible to NDV-GFP than the normal  
226 cells ranging from ~3.1x to ~78.7x. The oncolytic effect of NDV-GFP was more evident  
227 in the cell lines with mesenchymal-like morphology (M5, M25 and CF41.Mg) instead the  
228 cell lines with epithelial-like phenotype (E20 and E37).

229

230 **Table 1.** Cytotoxic effects of NDV in cancer cell lines and fibroblasts.

Cell line	Time to detect GFP in cell culture	IC <sub>50</sub> (MOI)	Selectivity index*
M5	~20h	0.12 ± 0.04	~78.7x
M25	~24h	0.17 ± 0.04	~56.1x
Cf41.Mg	~24h	1.54 ± 0.17	~6.2x
E37	~24h	2.03 ± 0.49	~4.7x
E20	~48h	3.08 ± 0.51	~3.1x
Fibroblasts	~24h	9.51 ± 2.39	~1x

231

232 \* In comparison to normal cells (fibroblasts)

233

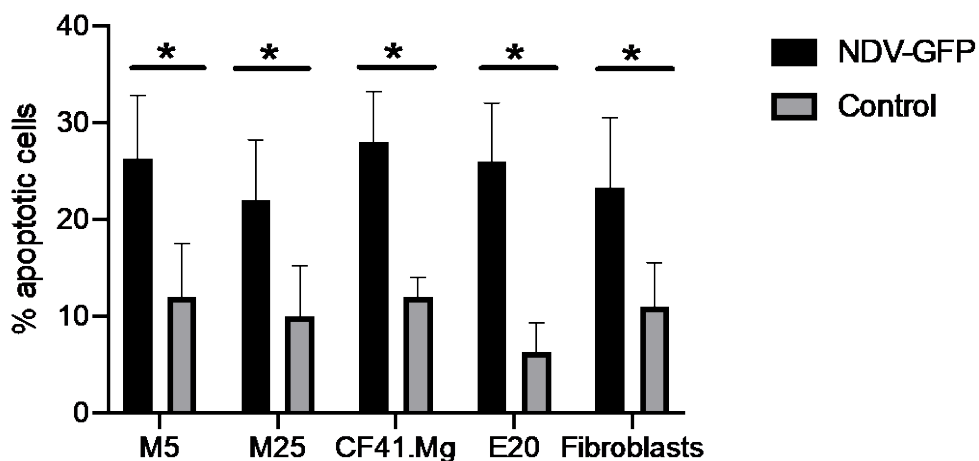
234

235 **Cell death induced by NDV-GFP**

236 We also analyzed which type of cell death the virus induced in cancer cells by  
237 double staining with acridine orange and ethidium bromide, which discriminates between  
238 apoptosis and oncolysis. The cell lines exposed to each IC<sub>50</sub> of NDV-GFP (including the

239 control cells) cells died exclusively by apoptosis ( $p<0.0001$ , fig.1) with no difference  
240 between cells lines ( $p=0.61$ ) due to the use of the IC50 for each cell line.

241



242

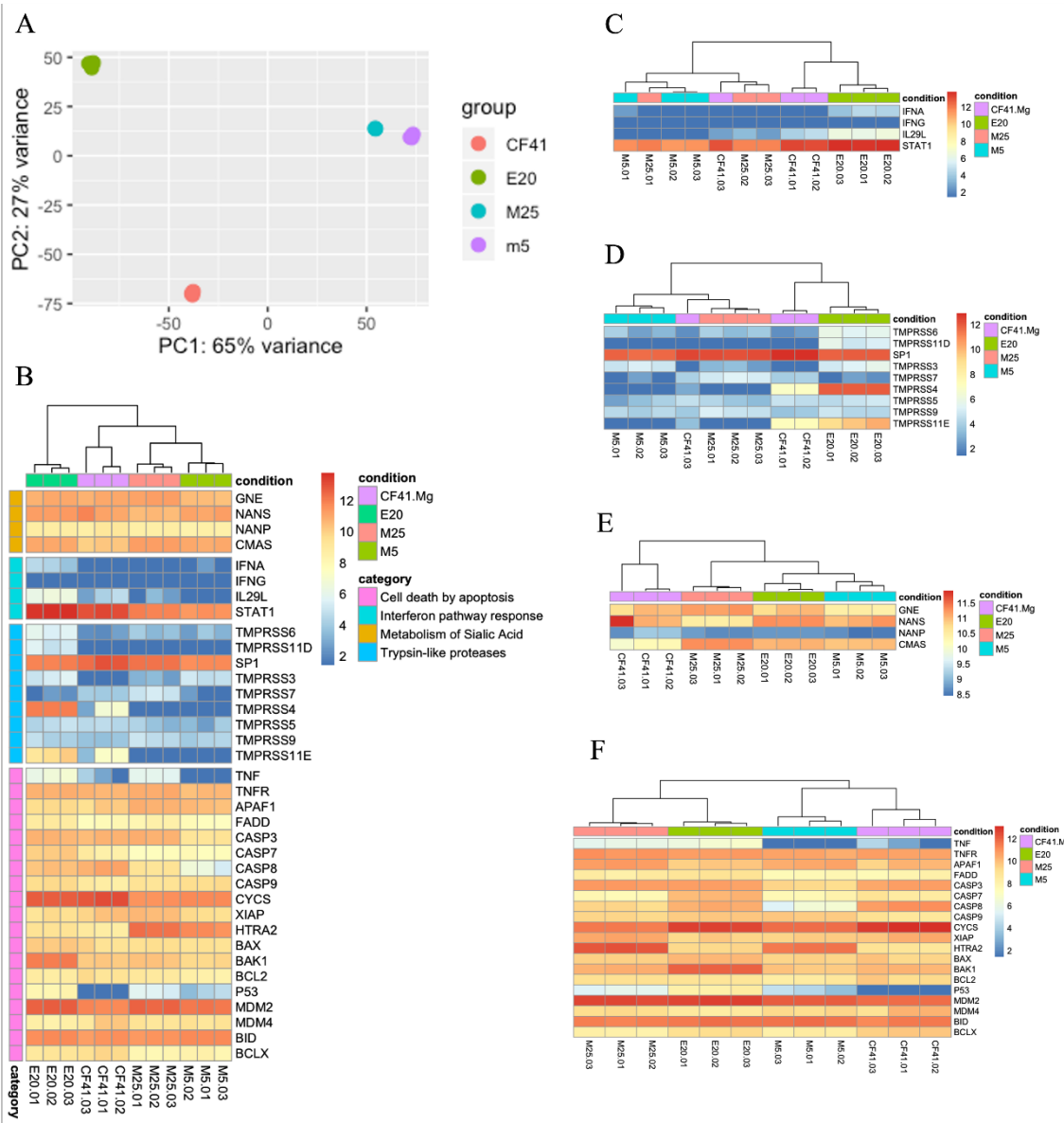
243 **Figure 1.** Induction of apoptosis in CMC cell lines by NDV-GFP. Cell lines were exposed  
244 to the IC50 and non-exposed (controls) were evaluated after 72 hours. The NDV exposure  
245 significantly induced cell death by apoptosis in all cells regardless of type (\*  $p<0.0001$ ).  
246

247

#### 248 Selectivity of NDV-GFP is inversely related to interferon pathway expression

249 Global gene expression PCA analysis showed that some cells are clearly different  
250 from each other (Figure 2A) being M25 and M5 more similar than CF41.Mg and E20.  
251 Next we selected representative genes from 4 biological processes associated with virus  
252 infection and cell response: metabolism of sialic acid (4 genes), trypsin-like proteases (9  
253 genes), interferon pathway (4 genes) and cell-death by apoptosis (19 genes). When we  
254 analyzed the expression of these 36 genes at the same time, cell types clustered according  
255 to the susceptibility to oncolytic effects (M5>M25>Cf41.Mg>E20, being the M5 the most  
256 susceptible) and a clusterization of mesenchymal-like cells occurred in opposition to the  
257 epithelial-like cancer cells (Fig. 2B). The four cell lines expressed similarly the genes of  
258 metabolism the sialic acid (Fig. 2E) but the majority of the trypsin-like proteases have  
259 low expression in these cancer cells (Fig. 2D) apart from the SP1 protease which was  
260 highly expressed in all cell lines. On the other hand, the less sensitive cell line (E20) to  
261 NDV oncolysis expressed more two proteases (TMPRSS4 and TMPRSS11E) than the  
262 more sensitive cell lines. The expression of genes from the interferon pathway response  
263 clustered the cell lines according to the oncolytic effects. Clearly the more sensitive cell  
264 line (M5) expressed significantly less *IFNA*, *IL29L* and also *STAT1* than the more

265 resistant cell line (E20, Figure 2C). Therefore, we proposed the IFN pathway as the most  
 266 important for the oncolytic effects of NDV in canine mammary cancer cells.  
 267



268  
 269 **Figure 2.** Transcriptome analysis of CMC cell lines. (A) Principal component analysis of  
 270 transcriptome from 4 CMC cell lines. Triplicates of each CMC cell line were analyzed.  
 271 This analysis considered all genes expressed in all CMC cell lines and showed distinction  
 272 between cell lines. Clearly, the E20 cell line was distinct from the mesenchymal cell lines.  
 273 (B) Heatmap from selected genes of 4 major pathways related to virus infection and cell  
 274 response. This analysis clustered all mesenchymal-like cells (CF41.Mg, M5 and M25) in  
 275 opposition to the epithelial-like cell line (E20) and supported the selectivity index to NDV  
 276 oncolysis. (C-F) Heatmaps based on genes related to metabolism of sialic acid (4 genes),  
 277 trypsin-like proteases (9 genes), interferon pathway (4 genes) and cell-death by apoptosis

278 (19 genes). Only the Interferon-pathway genes (C) clustered cells according to the  
279 selectivity index (M5>M25>Cf41.Mg>E20, being the M5 the most susceptible). The  
280 interferon genes were more expressed in the E20 cell line, the most resistant to oncolytic  
281 effects of NDV.

282

283

284 **Discussion**

285

286 In the present study, we studied the oncolytic effects of one lentogenic NDV strain  
287 in five canine mammary cancer cell lines and one non-tumorigenic fibroblast cell line,  
288 regarding cell viability, cell death, selectivity index, morphology and transcriptome  
289 analyses. We demonstrated a remarkable oncolytic effect of NDV-GFP in the mammary  
290 cancer cell lines and showed that the interferon pathway response was the most important  
291 for the susceptibility of NDV-GFP in cancer cells. Also, a strong selectivity index in more  
292 tumorigenic, mesenchymal-like cancer cells was demonstrated in comparison to other  
293 less tumorigenic and non-tumorigenic cells. Hence, these results support this NDV strain  
294 as a promising therapeutic option for clinical trials in canine patients.

295

296 The NDV is known for its oncolytic effects for a long time (ADAMS; PRINCE,  
297 1957; PRINCE; GINSBERG, 1957a, 1957b), but its use in canine patients was restricted  
298 to two studies so far (SANCHEZ. et al., 2014; SÁNCHEZ et al., 2015). There are several  
299 advantages to consider NDV a potential canine therapeutic option: the low virulence in  
300 dogs, several options of lentogenic strains available, established methods to produce the  
301 viral particles, relative cheap production and the possibility of gene editing by reverse  
302 genetics (CHENG et al., 2016). The direct oncolysis induced by paramyxoviruses in  
303 cancer cells are dependent of at least three different levels: the overexpression of sialic  
304 acid-containing sialoglycoproteins in cell surface; virus activation through cancer-  
305 specific proteases and; genetic defects of cancer cells that allowed virus replication as the  
306 loss of the ability to produce and respond to IFN and the induction of apoptotic pathways  
307 (MATVEEVA et al., 2015). In our work, we analyzed these mechanisms in canine cancer  
308 cells and showed a correlation of downregulation of IFN pathway and the selective  
309 oncolysis of NDV, demonstrating this mechanism as the most prominent for oncolysis by  
310 NDV. Interestingly, the less susceptible cell lines (E20 and E37) are less malignant, with  
311 an epithelial-like morphology and the more susceptible cell lines (M25, M5 and CF41)

312 are more malignant, with a mesenchymal-like morphology. The epithelial-mesenchymal  
313 transition is a fundamental oncogenic process improving the ability of cancer cells to  
314 migrate and metastasize, therefore, increasing the malignant potential of cancer cells.  
315 Interestingly, one work showed that EMT augmented the response to oncolytic  
316 herpesviral therapy (CHEN et al., 2014), suggesting that cancers exhibiting EMT may be  
317 naturally sensitive targets for herpesviral therapy. Although different viruses (herpesvirus  
318 x NDV) were used in different species (human x canine), our results supported that  
319 mesenchymal-like cancer cells are more susceptible to oncolytic virotherapy.

320

321 The two principal component analysis (PCA) explained 92% of the variance  
322 between 4 cell lines (E20, CF41, M5 and M25) and clearly demonstrated the epithelial-  
323 like cancer cell line (E20) is different than the other mesenchymal-like ones. The  
324 epithelial-like cancer cell line (E20) expressed more IFN pathway genes as *IFNA*, *IL29*  
325 and *STAT1* than the mesenchymal-like cells, but also certain apoptotic pathway genes as  
326 *P53*, *TNF* and the pro-apoptotic *BAK1* and also expressed two trypsin-like proteases the  
327 *TMPRSS4* and *TMPRSS11E*. Apparently, the sialic acid pathway is the less important  
328 process for oncolysis by NDV in our model since all cell lines expressed the genes in a  
329 similar way. In addition, no clear pattern of expression of trypsin-like proteases by cancer  
330 cells was noted since the less susceptible cells to NDV (E20) expressed more *TMPRSS4*  
331 and *TMPRSS11E* but was the last cell line to show virus infection (48h) for example.  
332 These results suggest that the pathways and genes related to antiviral response and/or  
333 virus infection were important to NDV selective oncolysis in our conditions. Thereby, if  
334 one ponders the future use of NDV for canine cancer it will probably be as a targeted  
335 therapy that will consider a panel of tumor gene expression prior to use due to the highly  
336 variable selectivity index.

337

338 The NDV-GFP used in this experiment induced apoptosis in a similar way in all  
339 cell lines, tumorigenic or not, when using the respective IC50 for each cell line, proving  
340 that NDV induced cell death mode of action is by apoptosis independently of the cell  
341 type. More exciting, is the high SI found in cancer cells ranging from  $\approx 3x$  up to  $\approx 79x$ ,  
342 especially in the more malignant cell lines; for comparison, a value of  $SI > 2$  is generally  
343 considered a high degree of selectivity (BADISA et al., 2009). The SI demonstrates the  
344 differential activity of a given substance and the greater the SI value is, the more selective

345 it is. This is a very important property for cancer therapeutics since the majority of the  
346 commercial cancer drugs have a very small therapeutic window.

347

348 To the best of our knowledge, this is the first description of oncolysis by an NDV  
349 strain in canine mammary cancer cells. We also demonstrated specific molecular  
350 pathways related to NDV susceptibility in these cancer cells, opening the possibility of  
351 using NDV as therapeutic-targeted option for more malignant CMCs. Therefore, these  
352 results greatly urge for more studies using oncolytic NDVs, especially considering  
353 genetic editing to improve efficacy in dogs and in humans.

354

355

## 356 **References**

- 357 ADAMS, W. R.; PRINCE, A. M. An electron microscopic study of incomplete virus  
358 formation; infection. **The Journal of experimental medicine**, v. 106, n. 5, p. 617–626,  
359 1957.
- 360 AL-GARIB, S. O. et al. Tissue tropism in the chicken embryo of non-virulent and  
361 virulent Newcastle diseases strains that express green fluorescence protein. **Avian**  
362 **Pathology**, v. 32, n. 6, p. 591–596, 12 dez. 2003. Disponível em:  
363 <<http://www.ncbi.nlm.nih.gov/pubmed/14676009>>. Acesso em: 29 out. 2018.
- 364 ANDERS, S.; PYL, P. T.; HUBER, W. HTSeq-A Python framework to work with high-  
365 throughput sequencing data. **Bioinformatics**, v. 31, n. 2, p. 166–169, 2015.
- 366 BADISA, R. B. et al. Selective cytotoxic activities of two novel synthetic drugs on  
367 human breast carcinoma MCF-7 cells. **Anticancer Research**, v. 29, n. 8, p. 2993–2996,  
368 ago. 2009.
- 369 CHEN, C. H. et al. Epithelial-mesenchymal transition enhances response to oncolytic  
370 herpesviral therapy through nectin-1. **Human Gene Therapy**, v. 25, n. 6, p. 539–551, 1  
371 jun. 2014.
- 372 CHENG, X. et al. Genetic Modification of Oncolytic Newcastle Disease Virus for  
373 Cancer Therapy. **Journal of Virology**, v. 90, n. 11, p. 5343–5352, 1 jun. 2016.  
374 Disponível em: <<http://jvi.asm.org/lookup/doi/10.1128/JVI.00136-16>>. Acesso em: 29  
375 out. 2018.
- 376 CORDEIRO, Y. G. et al. Transcriptomic profile reveals molecular events associated to  
377 focal adhesion and invasion in canine mammary gland tumour cell lines. **Veterinary**  
378 **and Comparative Oncology**, v. 16, n. 1, 2018.

- 379 DOBIN, A. et al. STAR: ultrafast universal RNA-seq aligner. **Bioinformatics**, v. 29, n.  
380 1, p. 15–21, jan. 2013.
- 381 ENGELAND, C. E.; BELL, J. C. Introduction to Oncolytic Virotherapy. In: **Methods**  
382 in **Molecular Biology**. [s.l.] Humana Press Inc., 2020. 2058p. 1–6.
- 383 GARCÍA-ALCALDE, F. et al. Qualimap: Evaluating next-generation sequencing  
384 alignment data. **Bioinformatics**, v. 28, n. 20, p. 2678–2679, 2012.
- 385 GONÇALVES, N. J. N. et al. Generation of LIF-independent induced pluripotent stem  
386 cells from canine fetal fibroblasts. **Theriogenology**, v. 92, 2017.
- 387 HALL, T. A. BIOEDIT: a user-friendly biological sequence alignment editor and  
388 analysis program for Windows 95/98/ NT. **Nucleic Acids Symposium Series**, v. 41, p.  
389 95–98, 1 jan. 1999.
- 390 KUMAR, S.; STECHER, G.; TAMURA, K. MEGA7: Molecular Evolutionary Genetics  
391 Analysis Version 7.0 for Bigger Datasets. **Molecular Biology and Evolution**, v. 33, n.  
392 7, p. 1870–1874, 22 mar. 2016. Disponível em:  
393 <<https://doi.org/10.1093/molbev/msw054>>.
- 394 LI, H. et al. The Sequence Alignment/Map format and SAMtools. **Bioinformatics**  
395 (**Oxford, England**), v. 25, n. 16, p. 2078–9, ago. 2009.
- 396 LOVE, M. I.; HUBER, W.; ANDERS, S. Moderated estimation of fold change and  
397 dispersion for RNA-seq data with DESeq2. **Genome Biology**, v. 15, n. 12, 5 dez. 2014.
- 398 MATVEEVA, O. V. et al. **Oncolysis by paramyxoviruses: Multiple mechanisms**  
399 **contribute to therapeutic efficiency****Molecular Therapy - Oncolytics****Nature**  
400 Publishing Group, , 22 jul. 2015. .
- 401 MILLER, P. J. et al. International Biological Engagement Programs Facilitate  
402 Newcastle Disease Epidemiological Studies. **Frontiers in Public Health**, v. 3, n. 9, p.  
403 235, 19 out. 2015. Disponível em:  
404 <<http://journal.frontiersin.org/Article/10.3389/fpubh.2015.00235/abstract>>. Acesso em:  
405 5 mar. 2020.
- 406 OIE. Newcastle Disease (infection with Newcastle disease virus). In: **Manual of**  
407 **diagnostic tests and vaccines for terrestrial animals: mammals, birds and bees.**  
408 Paris: World Organization for Animal Health, 2012. p. 555–574.
- 409 PRINCE, A. M.; GINSBERG, H. S. Studies on the cytotoxic effect of Newcastle  
410 disease virus (NDV) on Ehrlich ascites tumor cells. I. Characteristics of the virus-cell  
411 interaction. **J Immunol**, v. 79, n. 2, p. 94–106, 1957a. Disponível em:  
412 <<http://www.ncbi.nlm.nih.gov/pubmed/13475814>>. Acesso em: 2 mar. 2020.

413 PRINCE, A. M.; GINSBERG, H. S. Studies on the cytotoxic effect of Newcastle  
414 disease virus (NDV) on Ehrlich ascites tumor cells. II. The mechanism and significance  
415 of in vitro recovery from the effect of NDV. **Journal of immunology (Baltimore,**  
416 **Md. : 1950)**, v. 79, n. 2, p. 107–12, ago. 1957b. Disponível em:  
417 <<http://www.ncbi.nlm.nih.gov/pubmed/13475815>>. Acesso em: 2 mar. 2020.

418 REED, L. J.; MUENCH, H. A SIMPLE METHOD OF ESTIMATING FIFTY PER  
419 CENT ENDPOINTS12. **American Journal of Epidemiology**, v. 27, n. 3, p. 493–497,  
420 1 maio 1938. Disponível em: <<https://academic.oup.com/aje/article-lookup/doi/10.1093/oxfordjournals.aje.a118408>>. Acesso em: 29 out. 2018.

421 RIBBLE, D. et al. A simple technique for quantifying apoptosis in 96. **BMC**  
422 **Biotechnology**, v. 7, p. 1–7, 2005.

423 RUSSELL, S. J.; BARBER, G. N. Oncolytic Viruses as Antigen-Agnostic Cancer  
424 Vaccines. **Cancer cell**, v. 33, n. 4, p. 599–605, 2018. Disponível em:  
425 <<http://www.ncbi.nlm.nih.gov/pubmed/29634947>>. Acesso em: 14 out. 2019.

426 SANCHEZ., D. et al. In Vitro and in Vivo oncolytic Activity of Lasota Strain of  
427 Newcastle Disease Virus on a Lymphoma B-Cell Line and a Canine Cutaneous T-Cell  
428 Lymphoma. **Blood**, v. 124, n. 21, p. 5504–5504, 6 dez. 2014.

429 SÁNCHEZ, D. et al. Newcastle Disease Virus: Potential Therapeutic Application for  
430 Human and Canine Lymphoma. **Viruses**, v. 8, n. 1, p. 3, 23 dez. 2015. Disponível em:  
431 <<http://www.mdpi.com/1999-4915/8/1/3>>. Acesso em: 21 fev. 2020.

432 SÁNCHEZ, D. et al. Oncolytic Viruses for Canine Cancer Treatment. **Cancers**, v. 10,  
433 n. 11, p. 404, 27 out. 2018. Disponível em: <<http://www.mdpi.com/2072-6694/10/11/404>>. Acesso em: 21 fev. 2020.

434 SCHIRRMACHER, V.; VAN GOOL, S.; STUECKER, W. Breaking Therapy  
435 Resistance: An Update on Oncolytic Newcastle Disease Virus for Improvements of  
436 Cancer Therapy. **Biomedicines**, v. 7, n. 3, 30 ago. 2019. Disponível em:  
437 <<http://www.ncbi.nlm.nih.gov/pubmed/31480379>>. Acesso em: 14 out. 2019.

438 SLEECKX, N. et al. Canine mammary tumours, an overview. **Reproduction in**  
439 **domestic animals = Zuchthygiene**, v. 46, n. 6, p. 1112–31, dez. 2011. Disponível em:  
440 <<http://www.ncbi.nlm.nih.gov/pubmed/21645126>>. Acesso em: 14 out. 2019.

441 THOMPSON, J. D.; HIGGINS, D. G.; GIBSON, T. J. CLUSTAL W: improving the  
442 sensitivity of progressive multiple sequence alignment through sequence weighting,  
443 position-specific gap penalties and weight matrix choice. **Nucleic Acids Research**, v.  
444 22, n. 22, p. 4673–4680, 11 nov. 1994. Disponível em:

447 <<https://doi.org/10.1093/nar/22.22.4673>>.  
448 XAVIER, P. L. P. et al. ZEB1 and ZEB2 transcription factors are potential therapeutic  
449 targets of canine mammary cancer cells. **Veterinary and Comparative Oncology**,  
450 2018.  
451 ZAKAY-RONES, Z.; TAYEB, S.; PANET, A. Therapeutic potential of oncolytic  
452 Newcastle disease virus a critical review. **Oncolytic Virotherapy**, v. 4, p. 49, mar.  
453 2015.  
454  
455